ELECTRIC FIELD DETERMINATION IN WATER TREED SAMPLES USING THE THERMAL STEP METHOD

Cristina Stancu[1], P. V. Notingher[2], P. Notingher jr[3], M.Plopeanu[2]

[1] INCDIE ICPE CA, 313 Splaiul Unirii, P.O. Box 149, Bucharest 030138, Romania

[2] Politehnica University of Bucharest, Splaiul Independentei St.,

No.313, 060042, Bucharest, Romania

[3]Université Montpellier 2, Institut d'Electronique du Sud, Groupe Energie et Matériaux,

Place E. Bataillon, CC 083, 34095 Montpellier Cedex 5, France

Email: cstancu@icpe-ca.ro, petrunot@elmat.pub.ro, mgplopeanu@elmat.pub.ro,

petru@univ-montp2.fr

Abstract

In this paper a computation method of the electric field and ionic space charge density in plane insulations with water trees (using the Comsol Multiphysics software and the measured current I_m (t) with Thermal Step Method) is presented. A parabolic spatial variation of volume charge density, an exponential variation of the electric permittivity ε and a linear dependency of ε and the temperature variation coefficient of permittivity α_ε, with the water medium concentration in trees, are considered. For a tree with a known length, different values of charge density are considered and the electric field and the thermal step currents I_c (t) are determined. The currents I_c (t) and I_m (t) are compared and the volume of charge density and electric field for which I_c (t) is identical with I_m (t) are kept.

Key words: *insulation systems, electric field, space charge, water trees*

1. INTRODUCTION

One of the main causes of premature breakdown of medium and/or high voltage electrical insulation is the existence of local electric fields exceeding the inception values partial discharges and electrical treeing (Dissado et al., 1992). The local intensification of the electric field is due to conductor defects (sharp edges, protrusions etc), insulation delamination (due to thermal solicitations, vibrations etc), electrochemical trees (water, cooper) etc.

In the case of polyethylene insulated power cables, water trees develop in the vicinity of bulk defects (bow tie trees), or from inner or outer semi conducting layers (vented trees) and they appear under the shape of micro cavities filled with water connected by very thin micro channels (Chen et al., 1993; Steennis et al., 1990). Water treeing leads to ionic space charge formation (corresponding to the salt dissolved in water), inside and outside the treed regions, the quantity depending on the salt concentration in water, on water trees dimensions, frequency of the electric field etc (Takada, 1999; Chen et al., 2003; Ho et al., 2002).

In previous papers (Stancu, 2008; Stancu et al., 2009), correlations between the water trees length l_a and medium space charge density ρ_v have been shown. Electric field computations corresponding to the space charge in steady-state regime (Stancu, 2008) shown that the field value could reach up to 56 kV/mm, exceeding the dielectric strength of air in normal conditions (3.2 kV/mm), and may approach

the inception field of electrical trees (60 kV/mm, in the case of some cavities with very low pressure (Kuffel et al., 1984)).

In the present paper a computation method of the electric field and space charge on the basis of measured thermal step current is presented. A Comsol software is used and the dependencies of permittivity ε and coefficient of permittivity with temperature α_ε as a function of their medium values (corresponding to polyethylene and water) and water concentration in trees are take into consideration.

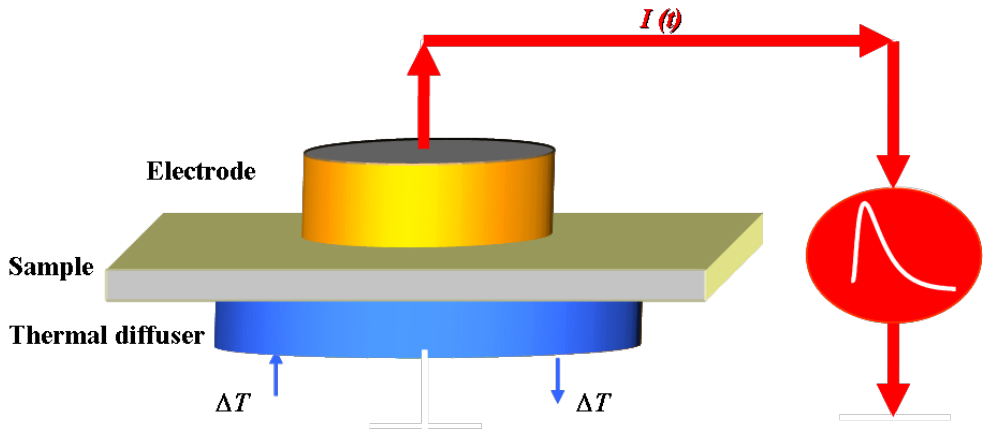

Figure 1. The setup used for the thermal wave current measurement

2. THERMAL STEP METHOD

The thermal step method (TSM) consists in the application of a thermal step ΔT (Fig.1) on one face of the tested sample situated between two electrodes (Toureille et al., 1990). As a consequence, the space charge inside the sample, moves, the induced charges on electrodes are modified, and by putting the electrodes in short-circuit a current appears, having the expression:

$$I(t) = -C\int_{y_0}^{y} \alpha_\varepsilon(y)E(y)\frac{\partial T(y,t)}{\partial t}\mathrm{d}y\,, \qquad (1)$$

where α_ε represents the permittivity variation factor with temperature, C – the sample capacity before the thermal step application, $E(y)$ – the electric field strength in coordinate point y (perpendicular measured on the electrodes surfaces), $T(y,t)$ – the temperature value in coordinate point y at instant t, y_0 – a computation value depending on the electrodes characteristics which is in contact with the liquid which generates the thermal wave (Cernomorcenco et al., 2008).

Using equation (1), the values of electric field $E(y)$ and volume space charge density $\rho_v(y)$ can be calculated in each point from the tested sample.

If in the case of homogeneous samples, ε and α_ε are known constants, their values are relatively difficult to determine in the case of water treed insulations. On the basis of some experimental data, different variations laws with the *y* coordinate have been proposed for ε: linear, parabolic, exponential etc (Radu et al., 1997; Acedo et al., 2001). In the present paper an exponential variation law of permittivity was considered (Radu et al., 2000):

$$\varepsilon_r(y) = ce^{-dy}, \tag{2}$$

where $\varepsilon_r(y)$ represents the relative permittivity in coordinate point *y*, *c* and *d* – material constants determined from the conditions:

$$\begin{aligned} &\varepsilon_r(y_0 + l_a) = \varepsilon_{rPE} \\ &\int_{y_0}^{y_0+l_a} \varepsilon_r(y)\mathrm{d}y = \varepsilon_{rm}.l_a \\ &\varepsilon_{rm} = c_{am}\,\varepsilon_{ra} + (1 - c_{am})\,\varepsilon_{rPE}, \end{aligned} \tag{3}$$

where l_a represents the tree length (assumed as continuous), c_{am} is the average water concentration of the tree and ε_{ra} and ε_{rPE} the relative permitivitties of water and polyethylene.

The α_ε coefficient values were deduced on the basis of permittivity variation curves of polyethylene (Alig et al., 2006; Svorcik et al., 2000) and water (Meissner et al., 2004) with temperature between -5 ºC si 25 ºC. The obtained values are $\alpha_{\varepsilon PE} = 4.4 \cdot 10^{-4}$ K^{-1} for polyethylene and $\alpha_{\varepsilon a} = -7.26 \cdot 10^{-3}$ K^{-1} for water.

For water treed regions a medium coefficient $\alpha_{\varepsilon m}$ was calculated:

$$\alpha_{\varepsilon m} = c_{am}\alpha_{\varepsilon a} + (1 - c_{am})\alpha_{\varepsilon PE}. \tag{4}$$

For a water concentration c_{am} = 1 % (Ross, 1998), it was obtained $\alpha_{\varepsilon m} = 3.63 \cdot 10^{-4}$ K^{-1}.

3. ELECTRIC FIELD COMPUTATION

Let us consider a flat sample which has the diameter *d* and the thickness *g*, situated between the ground electrode and the thermal diffuser (Fig. 1). It is supposed that from the sample face which is in contact with the thermal diffuser a continuous water tree with the length l_a has developed, to whom corresponds an ionic space charge layer of thickness $l_s > l_a$. This charge generates an electric field of intensity *E*. As the electric field has a plane parallel symmetry, it can be computed in a rectangular domain *D* (resulting from the division into sections of the disc with a perpendicular plane on its basis). The domain *D* is constitued of 4 sub domains $D_{1...4}$, delimited by the boundaries 1…13 (Fig. 2):

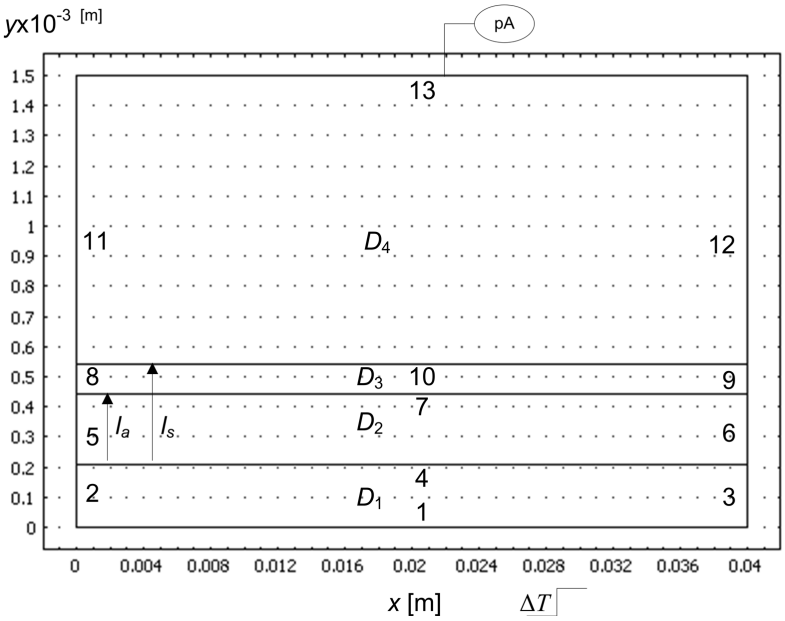

Figure 2. Computational domain of the electric field

- Sub domain D_1 - corresponds to the thermal diffuser/sample, whose thickness y_0 is experimentally determined. The electric field in zero in this sub domain;

- Sub domain D_2 - corresponds to the water treed region with the length l_a ($\varepsilon_r(y) = (1+\alpha_\varepsilon(T - T_0))\cdot ce^{-dy}$) and with a space charge layer with the thickness l_s - l_a and $\rho_v(y) = \rho_{v0}(ay^2 + by + e)$;

- Sub domain D_3 - corresponds to the region without trees ($\varepsilon_r(y) = \varepsilon_{rPE}(1+\alpha_\varepsilon(T - T_0))$) and a space charge layer with the thickness l_s and $\rho_v(y) = \rho_{v0}(ay^2 + by + e)$;

- Sub domain D_4 - corresponds to the region without water trees ($\varepsilon_r(y) = \varepsilon_{rPE}(1+\alpha_\varepsilon(T - T_0))$) and without space charge.

Considering that y_0, l_a, l_s, ρ_{v0}, a, b, c, α_ε, c, d, and g are known, using the Comsol Multiphysics software, the electric field repartition and temperature in domain D were determined. In this content, the Poisson equation for electric field $\Delta V = -\rho_v/\varepsilon$ and Fourier equation for temperature $\overline{q} = -\lambda \mathrm{div} T$ were solved, knowing the initials and boundaries conditions for electric potential $V(y)$ and temperature $T(y,t)$, and material constants.

In all sub domains, an initial temperature of 25 °C was considered. At the instant $t = 0$, the temperature on boundary 1 decreases to -5 °C, corresponding to the application of a thermal step $\Delta T = -30$ °C. It is considered that the thermal wave acts during $t = 5$ s, divided into $\Delta t = 5$ ms intervals.

The boundaries conditions are:

- $V = 0$ on boundaries 1,2,3,4 and 13;
- $\overline{nE} = 0$ on boundaries 5,6,8,9,11 and 12;

- $(\varepsilon E_n)_2 = (\varepsilon E_n)_3$ on boundary 7 and $(\varepsilon E_n)_3 = (\varepsilon E_n)_4$ on boundary 10.

where $\bar{n}$ is the surface normal and E_n the normal component of E.

For material constants, the following values have been considered: thermal conductivity λ = 0.38 W/mK, density γ = 930 kg/m^3, specific heat c_p = 1900 J/kgK, $\alpha_{\varepsilon PE} = 4.4 \cdot 10^{-4}$ K^{-1}, $\alpha_{\varepsilon a} = -7.26 \cdot 10^{-3}$ K^{-1}, $\alpha_{\varepsilon m} = 3.63 \cdot 10^{-4}$ K^{-1} and l_a = 227 μm.

The thermal step current corresponding to each case was computed using the relation

$$I_c(t) = -\varepsilon S \frac{dE_1}{dt}, \tag{5}$$

where ε is the absolute permittivity of sample, S is the electrode area and E_1 is the electric field strength in the vicinity of measuring electrode (Stancu, 2008).

4. EXPERIMENTS

4.1. Samples

The experiments were made on flat samples having the dimensions 100·100·0.5 mm^3, made from LDPE pellets (supplied by the Borealis Group) by pressmoulding at p = 200 bar and T = 145°C. In the samples, water trees (with different lengths l_a) were developed in an accelerated manner. For thermal step currents measurement, graphite electrodes (40 mm in diameter) have been deposited. After the measurement, the samples were cut in slices of 200 μm for the water trees lengths determination.

4.2. Setups

The setup used for water trees development is presented in figure 3 (Stancu, 2008). The applied voltage was U = 2 kV, the frequency f = 5 kHz, the NaCl concentration in water c = 0.1 mol/l, and the duration of voltage application τ = 0…48 h. The experimental setup from figure 4 was used for measuring the dimensions of the water trees.

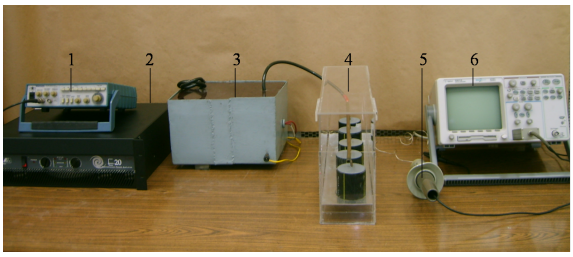

Figure 3. Setup used for accelerated water tree development:
(1) – Generator, (2) – Amplifier, (3) – Transformer,
(4) – Sample holder, (5) – Probe, (6) – HP Scope

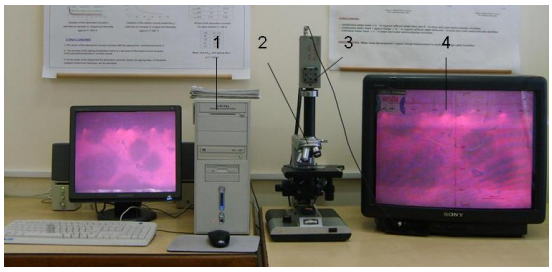

Figure 4. Setup used for measuring the dimensions of the water trees:
(1) – PC, (2) – Microscope, (3) – Camera, (4) – Monitor

5. RESULTS. DISCUSSIONS

5.1. Thermal step current measurement

The variations of the thermal step currents in samples without and with water trees are presented in Figure 6. In Table 1, the measured values of water tree length l_a (Fig. 5) and the maximum values of thermal step current $I_{m,\max}$ in un-aged and aged samples for different ageing time values τ are presented.

It can be observed that the maximum values of thermal step currents are higher in water treed samples with respect to virgin samples. This is due to space charge accumulation (along with the development of water trees), as a consequence of ions penetration (resulted from the dissociation of NaCl molecules) in the samples.

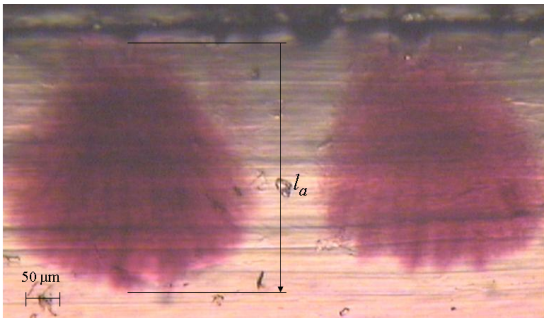

Figure 5. Water trees developed in LDPE samples
(τ = 48 h, U = 2 kV, f = 5 kHz, 0.1 mol/l NaCl)

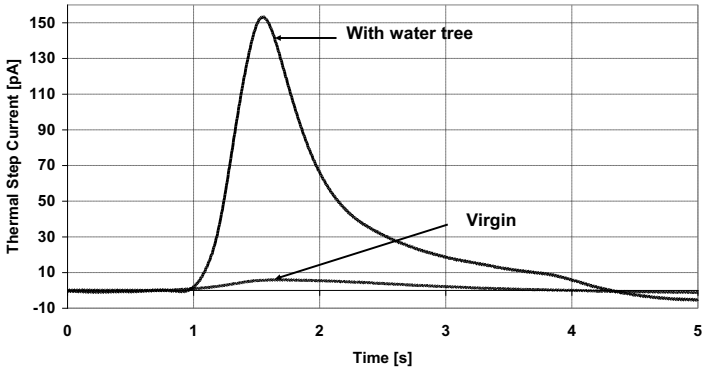

Figure 6. Thermal step currents $I_m(t)$ measured on samples without and with water trees (τ = 48 h, U = 2 kV, f = 5 kHz, 0.1 mol/l NaCl)

Table 1 - Water trees lengths l_a and thermal step currents $I_{m,max}$ values for different ageing time values τ.

τ [h]	l_a [µm]	$I_{m,max}$ [pA]
0	0	8
24	156.8	44
48	226.9	152

5.2. Computation of thermal step currents and electric field

Considering different values of ρ_{v0} (ρ_{v0} = - 4.4…- 1.3 C/m^3) and l_s (l_s = 267…327 µm), thermal step currents $I_c(t)$ for values of t between 0 and 5 s were computed using the Comsol software. The obtained curves $I_c(t)$ were compared with the experimental one $I_m(t)$ to find the values of ρ_{v0} and l_s for which $I_m(t) \approx I_c(t)$.

Figure 7 shows the variation of the maximum values of electric field strength E with ρ_{v0} and l_s. It can be observed that E_{max} decreases with the increase of l_s and increases with ρ_{v0}, variations which are similar to the one obtained in the case of medium voltage cables (Stancu, 2008).

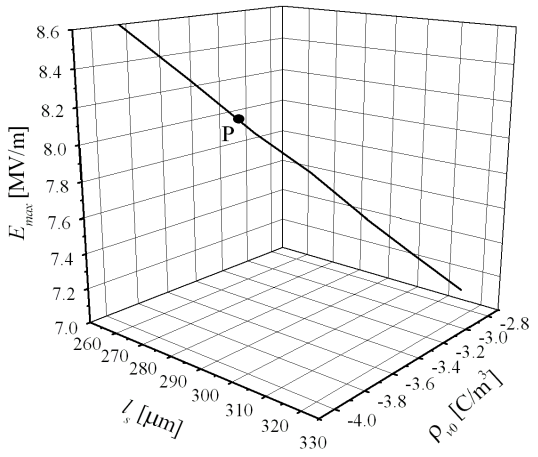

Figure 7. Maximum electric field E_{max} vs l_s and ρ_{v0} (l_a = 227 μm, $\alpha_{\varepsilon m} = 4.4 \cdot 10^{-4}$ K^{-1}, y_0 = 0.21 mm)

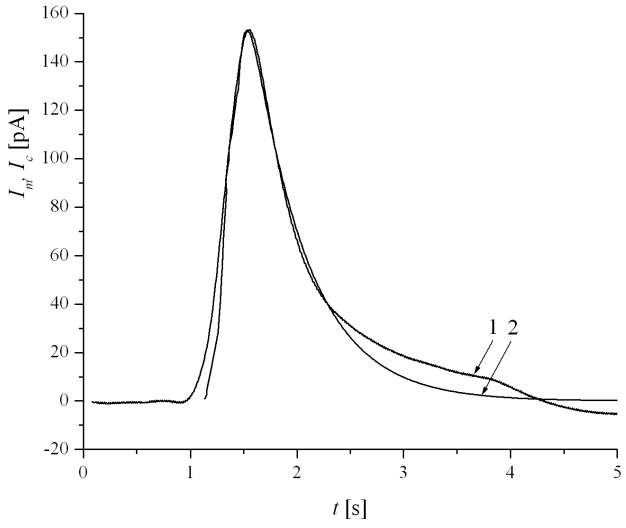

Figure 8. Measured I_m (1) and computed I_c (2) thermal step currents for ρ_{v0} = - 2.25 C/m^3 and $\alpha_{\varepsilon m} = 4.4 \cdot 10^{-4}$ K^{-1}or ρ_{v0} = - 3.35 C/m^3 and $\alpha_{\varepsilon m} = 3.63 \cdot 10^{-4}$ K^{-1} (l_a = 227 μm, l_s = 327 μm, y_0 = 0.21 mm)

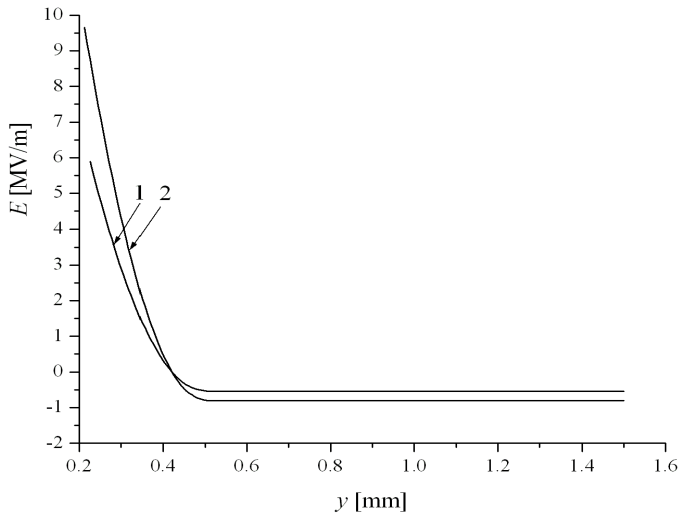

Figure 9. Electric field E variation vs y-coordinate for ρ_{v0} = - 2.25 C/m^3 and $\alpha_{\varepsilon m}$ = 4.4 ·10^{-4} K^{-1} (1) and ρ_{v0} = - 3.35 C/m^3 and $\alpha_{\varepsilon m}$ = 3.63 ·10^{-4} K^{-1} (2) (l_a = 227 μm, l_s = 327 μm, y_0 = 0.21 mm)

Figure 8 presents the thermal step current $I_m(t)$ measured experimentally on a water treed sample along with the thermal step current $I_c(t)$ simulated in water treed samples for which we have assumed l_a = 227 μm, l_s = 327 μm, y_0 = 0.21 mm and ρ_{v0} = - 2.25 C/m^3 and α_ε = 4.4 ·10^{-4} K^{-1}, or ρ_{v0} = - 3.35 C/m^3 and $\alpha_{\varepsilon m}$ = 3.63 ·10^{-4} K^{-1}. It can be observed that the decrease of the values of α_ε, due to water penetration inside the samples, leads to the increase of space charge density ρ_{v0} (from - 2.25 C/m^3 in the absence of the trees to - 3.35 C/m^3 in their presence).

For both values of $\alpha_{\varepsilon m}$, in figures 9 and 10 the variations of electric field and volume space charge density as a function of y are presented. It can be observed that the electric field strength E and volume space charge density have important variations in the vicinity of the regions from which the trees develop, and decrease with the y-coordinate, as a consequence of the decrease of ion concentration related to water trees (Visata, 2001).

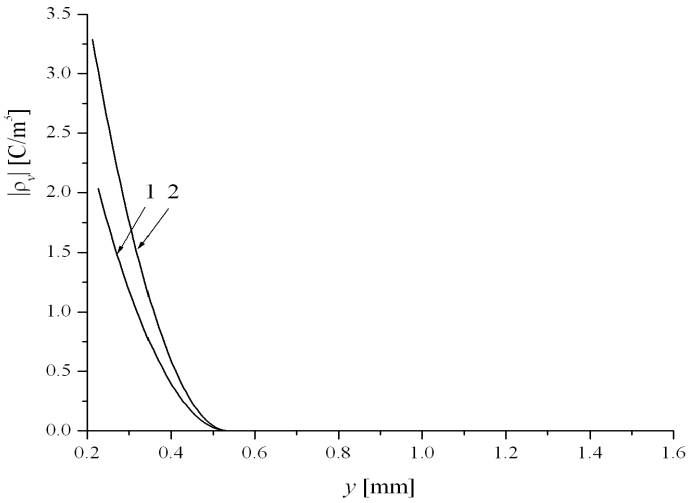

Figure 10. Volume space charge density ρ_v vs y-coordinate for ρ_{v0} = - 2.25 C/m^3 and $\alpha_{\varepsilon m}$ = 4.4 ·10^{-4} K^{-1} (1) and ρ_{v0} = - 3.35 C/m^3 and $\alpha_{\varepsilon m}$ = 3.63 ·10^{-4} K^{-1} (2) (l_a = 227 μm, l_s = 327 μm, y_0 = 0.21 mm)

It must be also remarked that the values of residual electric field in the vicinity of samples faces from where water trees develop are relatively important (10 kV/mm in the case of a tree with a medium water concentration 1 %), and increases if the water concentration increases (due to the increase of space charge density related to water trees). For example, if the average water concentration in the trees reaches 2.4 %, the value of E_{max} reaches to 56 kV/mm (enough to initiate electrical treeing).

6. CONCLUSIONS

The computational method presented evaluates in a good manner the residual electric field in water treed flat samples. The maximum values of the electric field depend on the space charge layer thickness l_s and on the volume space charge density.

The increase of water content in the trees results in an increase of maximum values of charge density ρ_{v0} and electric field E_{max}.

The computation of the residual electric field and space charge were made for an average value of permittivity variation factor α_ε with temperature. The influence of α_ε with respect to the y-coordinate on the residual electric field repartition will be presented in a future paper.

ACKNOWLEDGEMENT

This work was supported in part by the Romanian Ministry of Education, Research and Youth, PNCDI II Program – CABDIAG 22-122/2008.

REFERENCES

1. Dissado L.A., Fothergill J.C. Electrical Degradation and Breakdown in Polymers, Peter Pelegrinus, (London) 1992.
2. Chen J.L., Filipini J.C. The morphology and behavior of the water tree, IEEE Trans. on Diel. and Electr. Insul. 1993; 28: 271-86.
3. Steennis E., Kreuger F.H. Water treeing in polyethylene cables, IEEE Trans. on Diel. and Electr. Insul. 1990; 35: 989 -1028.
4. Visata O. Influence des arborescences d'eau sur les propriétés diélectriques des polymères, PhD Dissertation (UPB-UJF) 2001.
5. Takada T. Acoustic and optical methods for measuring electric charge distributions in dielectrics**,** IEEE Trans. on Diel. and Electr. Insul. 1999; 6: 519-47.
6. Chen G., Fu M. and Liu X.Z. Influence of AC ageing on space charge dynamics in LDPE, XIIIth International Symposium on High Voltage Engineering 2003; 8: 365.
7. Ho Y, Chen G., Davies A., Swingler E., Sutton S., Hampton N., Hobdell S. Measurement of space charge in XLPE insulation under 50 Hz AC electric stresses using the LIPP method , IEEE Trans. on Diel. and Electr. Insul. 2002; 9: 362-70.
8. Stancu C. Caracterisation de l'etat de vieillissement des isolations polymeres par la mesure d'arborescences et de charges d'espace, PhD Dissertation (UPB-UM2) 2008.
9. Stancu C.**,** Notingher P.V., Ciuprina F., Notingher jr P., Agnel S., Castellon J., Toureille A. Computation of the Electric Field in Cable Insulation in the Presence of Water Trees and Space Charge, IEEE Trans. on Ind. Appl. 2009; 45: 30-43.
10. Kuffel E., Zaengle W. S. High Voltage Engineering, Pergamon Press 1984.
11. Toureille A., Sabir A., Reboul J., Berdala J., Merle P. Determination des densites de charge d'espace dans un cable haute tension a forte epaisseur d'isolant par la methode de l'onde thermique, Revue de Physique Appliquee 1990; 25: 405-8.
12. Cernomorcenco A., Notingher jr P. Application of the thermal step method to space charge measurements in inhomogeneous solid insulating structures: A theoretical approach, Applied Physical Letters 2008; 93.
13. Radu I., Acedo M., Notingher P.V., Frutos F., Filippini J.C. The Danger of Water Trees in Polymer Insulated Power Cables Evaluated from Calculations of Electric Field in the Presence of Water Trees of Different Shapes and Permittivity Distributions, Journal of Electrostatics 1997; 40-41: 343-7.
14. Acedo M., Radu I., Frutos F., Filippini J.C., Notingher P.V. Water Treeing in Underground Power Cables: Modelling of the Trees and Calculation of the Electric Field Perturbation, Journal of Electrostatics 2001; 53: 267-94.
15. Radu I., Acedo M., Filippini J.C., Notingher P.V., Frutos F. The Effect of Water Treeing on the Electric Field Distribution of XLPE: Consequences on the Dielectric Strength, IEEE Trans. on Diel. and Electr. Insul. 2000; 7: 860-8.

16. Alig I., Dudkin S.M., Jenninger W., Marzantowicz M. AC Conductivity and Dielectric Permittivity of Poly(EthyleneGlycol) During Crystallization: Percolation Picture 2006; 47: 1722-31.

17. Svorcik V., Ekrt O., Rybka V., Liptak J., Hnatowicz V. Permittivity of Polyethylene and Polyethylenetereftalate, Journal of Materials Science Letters 2000; 19: 1843-45.

18. Meissner T., Wentz F.J. The complex dielectric constant of pure and sea water from microwave satellite observations, IEEE Trans. Geosci. Remore Sensing 2004; 42:1836-49.

19. Ross R. Inception and Propagation Mechanisms of Water Treeing, IEEE Trans. on Diel. and Electr. Insul. 1998; 5: 660-80.